J Seismol (2018) 22:519–537
https://doi.org/10.1007/s10950-017-9716-7

REVIEW ARTICLE

Tutorial review of seismic surface waves' phenomenology

A.L. Levshin · M. P. Barmin · M.H. Ritzwoller

Received: 1 June 2017 / Accepted: 15 November 2017 / Published online: 7 December 2017

Abstract In recent years, surface wave seismology has become one of the leading directions in seismological investigations of the Earth's structure and seismic sources. Various applications cover a wide spectrum of goals, dealing with differences in sources of seismic excitation, penetration depths, frequency ranges, and interpretation techniques. Observed seismic data demonstrates the great variability of phenomenology which can produce difficulties in interpretation for beginners. This tutorial review is based on the many years' experience of authors in processing and interpretation of seismic surface wave observations and the lectures of one of the authors (ALL) at Workshops on Seismic Wave Excitation, Propagation and Interpretation held at the Abdus Salam International Center for Theoretical Physics (Trieste, Italy) in 1990–2012. We present some typical examples of wave patterns which could be encountered in different applications and which can serve as a guide to analysis of observed seismograms.

Keywords Surface waves · Crustal structure · Ambient noise · Lithospheric structure

A. Levshin (✉) · M. P. Barmin · M. Ritzwoller
Center for Imaging the Earth's Interior, Department of Physics, University of Colorado at Boulder, Boulder, CO 80309-0390, USA
e-mail: levshin@colorado.edu

1 Introduction

Surface waves form the longest and strongest parts of seismic oscillations generated by explosions, external impacts on the Earth's surface, and shallow earthquakes. They also dominate in seismic ambient noise produced by microseisms. Traversing areas with diverse geological structures, surface waves absorb information of the properties of these areas. This information is best reflected in dispersion, the dependence of velocity on frequency. The other properties of these waves—such as polarization, frequency content, attenuation, azimuthal variation of the amplitude and phase—are also controlled by the medium between the source and receiver. Some of these are affected by the properties of the source and the geological conditions nearby, as well as by the conditions around the receiver. The information about the Earth structure and the seismic source contained in surface waves can be extracted from seismic records and applied to resolve numerous scientific and practical problems.

We mention some of these applications here:

- Determination of regional crustal, lithospheric, and upper mantle elastic/anelastic structure.
- Reconnaissance of sedimentary basins on land and seas.
- Survey of loose sediments and evaluation of static corrections for seismic prospecting goals, especially in multicomponent surveys, using PS reflections.

- Determination of the structure and elastic/anelastic properties of the shallow subsurface in various civil engineering, archeological, and environmental studies.
- Source characterization, including determination of magnitude, moment tensor, and dynamic parameters of the source, including size of rupture, direction, and speed of rupture propagation.
- Discrimination of underground nuclear explosions among various seismic events of both natural and human origin.
- Location of seismic events using ambient noise.

More information about different applications, including frequency ranges and depths of penetration, may be derived from Table 1. Diversity of various applications and corresponding frequency ranges (as well as geological conditions and excitation sources) makes phenomenology of surface waves quite complicated and deserving of special consideration. We will briefly describe a well-accepted technique for the analysis of surface wave records and present a series of examples of surface wave phenomenology in different applications.

2 Surface wave analysis

The dispersive properties and multi-mode character of surface waves make one-dimensional representations of their records in the time or frequency domain inefficient for measurements of the main parameters of the signals. A two-dimensional representation of the records in frequency–time diagrams permits separation of desired signals from other waves, as well as noise, and also allows measurement of their kinematic and dynamic characteristics. The current popular measurement procedures, known as FTAN (frequency–time analysis), are based on a long history of development of surface wave analysis (e.g., Dziewonski et al. 1969, 1972; Levshin et al. 1972, 1992, 1994; Levshin et al. 1989; Cara 1973; Russell et al. 1988). The recent innovation is that software has been developed which allow measurements to be made rapidly on relatively large volumes of data from heterogeneous networks and a variety of source regions. These innovations have required the development of rational parametric and waveform database structures and relatively rapid graphical routines for human interaction with the data (Ritzwoller et al. 1995; Ritzwoller and Levshin 1998). The general form of the measurement procedure is as follows: group velocity-period diagrams for vertical, radial, and transverse components are constructed using a computer-simulated system of narrow-band Gaussian filters (see Fig.1).

The analysis of these diagrams is made either in a dialog form or by an automated algorithm based on a dialog experience (Bensen et al. 2007, http://ciei.colorado.edu/Products). The presumed signal is selected by tracing the maximum amplitudes in the group time–period plane, collapsed into an impulsive signal by phase-matched filtering (Russell et al. 1988), then extracted from the original record by frequency–time tapering, and converted to the time domain by returning the introduced corrections to its phase spectrum. Then, amplitude and phase spectra of the cleaned signal are used to determine their kinematic and dynamic characteristics. In what follows, we discuss applications of this technique in different surroundings and different frequency ranges.

The group velocity measurements are practically free of problems related to the source phase (Levshin et al. 1999), polarity of instruments, etc. FTAN also provides

Table 1 Surface waves in the Earth's studies

Frequency (Hz)	Period (s)	Wave length (km)	Phase velocity (km/s)	Penetration (km)	Applications
10–50	0.02–0.1	0.002–0.05	0.1–0.5	0.020	Static corrections, civil engineering, ecology, archeology
0.1–0.2	5–10	7–30	2–3	5	Static corrections, loose sediments' studies
0.03–0.1	10–35	30–100	3.0–3.5	10	Crustal studies
0.003–0.03	35–350	200–1000	4–5	300	Upper mantle's studies
0.2–0.7	5–15	10–50	2.0–3.5	30	Epicenter's location

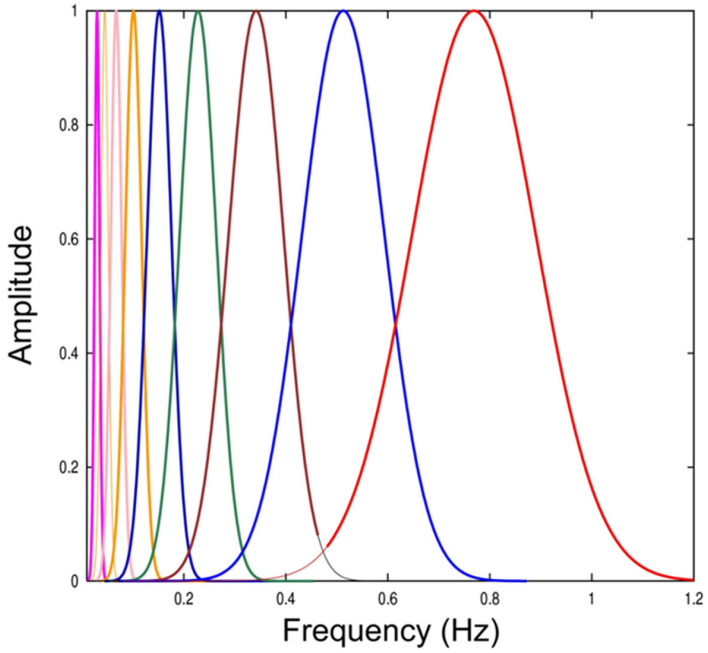

Fig. 1 The system of narrow-band Gaussian filters used in many versions of the frequency–time analysis

phase information which can be used for phase velocity measurements, after correction for the source phase and other phase corrections depending on the type of experiment. Both types of velocities are widely used now in various seismological studies. The advanced version of FTAN allows polarization measurements which helps to separate Rayleigh and Love waves, and the determination of their azimuths of approach to the receivers and the ellipticity of the Rayleigh waves (Levshin et al. 1989, 1992).

3 Surface waves: continental scale

Due to the high average efficiency of surface wave propagation across continents, surface wave measurements can be made at periods of up to 100–150 s for earthquakes as small as Ms = 5.0 propagating across the entire continent. Of course, measurements can be extended to longer periods for substantially larger events. As an example, group velocity measurements for a single station (KEVO, Finland) for one event (Kuril event, October 9, 1994, Ms = 7.0) are shown in Fig.2 for the Rayleigh wave (measured on the vertical and radial components) at periods of between about 20 and 300 s and for the Love wave at periods between about 30 and 250 s. Predictions for the spherical model PREM (Dziewonski and Anderson 1981) are shown for comparison.

4 Surface waves: regional scale

On a regional scale at shorter periods, smaller events (Ms < 5.0) can be analyzed similarly (Levshin & Ritzwoller 2001). KNET (Kyrgyzian Digital Network) (Vernon 1994), situated in a complex tectonic setting in Central Asia and surrounded to the East, West, and South by significant seismicity, is a natural site to focus on studies of regional scale measurements. Distances between KNET stations are less than 200 km. Due to complexity of the region, records of KNET stations are usually quite complicated and exhibit a great variety of wave patterns from the same event across this array and from one event to another. Figure 3 presents an example of an analysis of

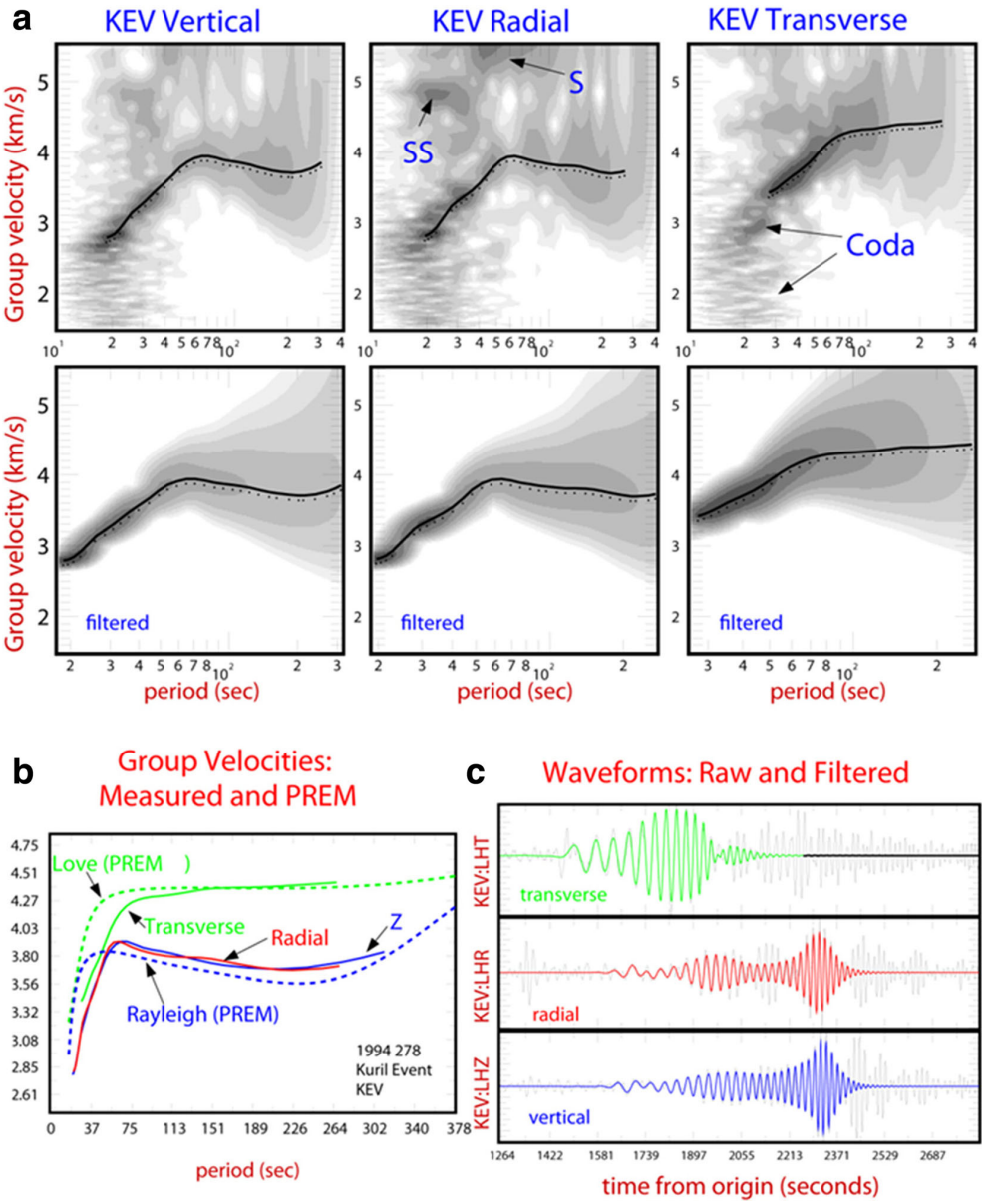

Fig. 2 Example of group velocity measurements for the fundamental modes of Rayleigh and Love waves across Eurasia. **a** Raw and filtered FTAN diagrams. **b** Group velocities. **c** Raw and filtered waveforms from the Kuril event on October 9, 1994 recorded by station KEVO (Finland) at the epicentral distance 6534 km

records obtained at KNET stations during the passage of surface waves from an event in the Qinghai Province, China on January 27, 1994 (epicentral distances are ~1890 km, Ms = 4.8). Rayleigh and Love wave FTAN diagrams are shown in Fig.3a, resulting in group velocity curves (shown in Fig. 3b). The raw and filtered waveforms are presented in Fig.3c. It appears that the Rayleigh wave measurements are quite similar across the array above a period ~20 s and for Love waves above a period ~30 s for this azimuth of approach. Variations across the array at short periods

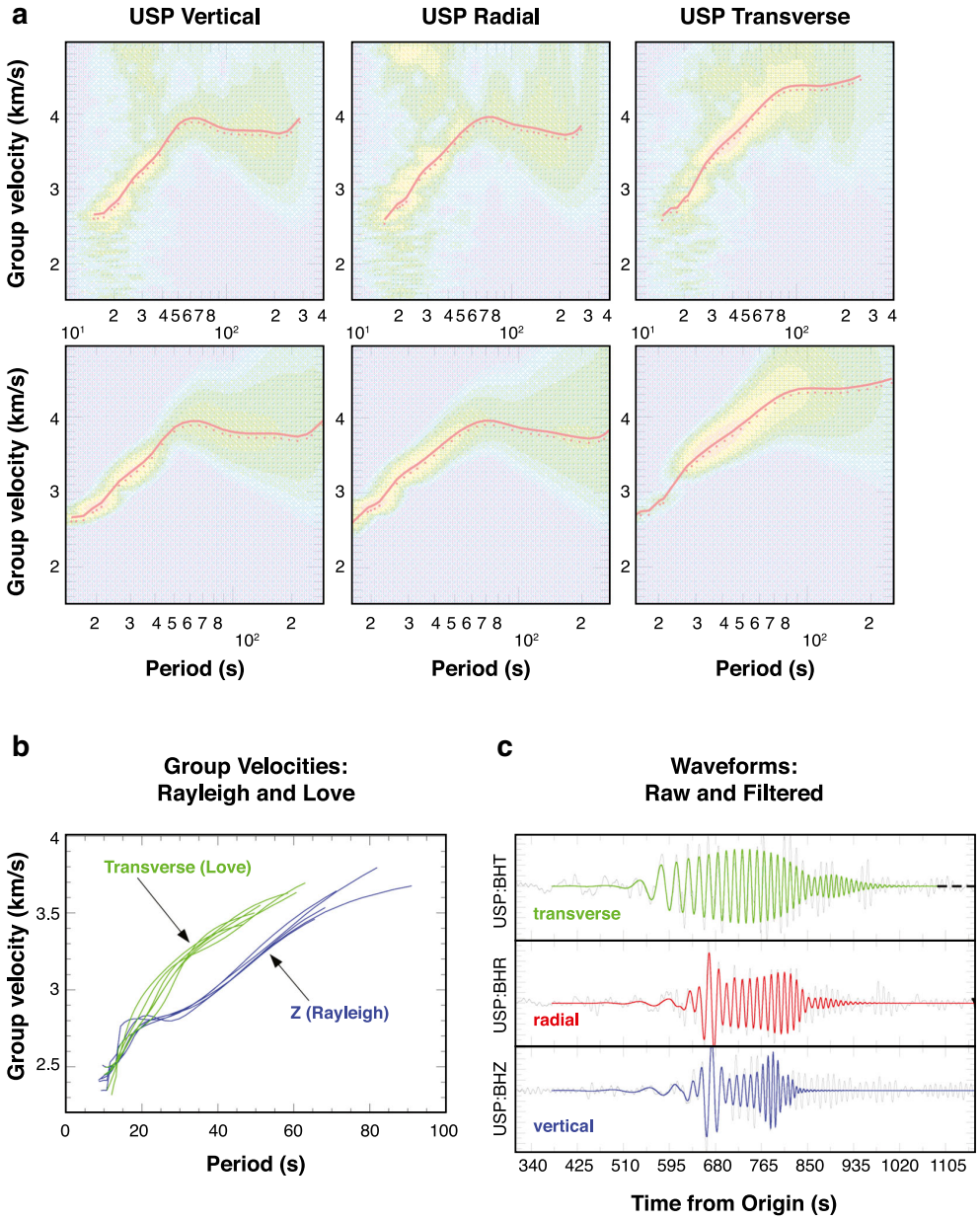

Fig. 3 Group velocity measurements for the fundamental modes of Rayleigh and Love waves from a regional event (Western China, January 27, 1994, Ms = 4.8) recorded by stations of the KNET array (Kyrgyzstan). **a** Raw and filtered FTAN diagrams. **b** Resulting group velocity curves obtained at 5 stations. **c** Raw and filtered waveforms for USP station

result both from real differences for the various wave paths near the network and from Rayleigh–Love interference, which can be significant since the group velocities of the two wave types are similar in this period range.

5 Surface waves at the ocean

Significant differences exist in surface wave propagation along oceanic and continental paths. There are at least three reasons for this:

(1) Presence of ~4 km of water in the ocean. Love wave (as a shear wave) ignores the water layer. The fundamental Rayleigh mode propagates partly in water and is significantly slowed at short periods by this low-velocity layer. Higher Rayleigh modes are not sensitive to water.
(2) The Earth's crust is significantly thinner in the oceans (5–10 km) than at continents (30–50 km) and composed mostly by basalts (i.e., higher average velocities than in a continental crust).
(3) The oceanic lithosphere is, in general, more laterally homogeneous than the continental lithosphere.

Differences in kinematic characteristics of fundamental modes of surface waves at oceanic and continental models are shown in Fig.4.

An example of surface wave propagation across the Pacific Ocean is shown in Fig.5. Note a strong scatter of short-period waves (7–12 s) along the oceanic paths (seen as gray spots on FTAN diagrams) and its practically being absence along the continental path (Fig.2).

Note, also, some "footprints" of Love waves at the vertical component and Rayleigh waves at the transverse component, in contradiction to the theoretical prediction for a laterally homogeneous, isotropic Earth. (This phenomenon will be discussed later.) Very often, we observe waves whose paths include both continental and oceanic parts and seas with oceanic lithosphere structures. The observed group velocities have intermediate values between continental and oceanic velocities. Due to the scattering effect of continental margins, short-period parts of surface wave signals strongly attenuate when crossing these zones.

6 Surface waves in sedimentary basins

If the paths of surface waves cross significant sedimentary basins, their travel times noticeably decrease in comparison with travel times for paths which do not cross such regions. For example, strong anomalies are observed for paths crossing the Northern Caspian Sea and the Pre-Caspian Depression (Berteussen et al. 1983), the Barents Sea shelf (Levshin and Berteussen 1979), the Laptev Sea (Lander 1989b), the Tarim Basin (Levshin et al. 2005), the Mexican Gulf (Shapiro and Ritzwoller 2002), and a number of other basins. The effect of a thick sedimentary basin on Rayleigh wave group velocity is shown in Fig.6.

The effect of the Barents Sea sedimentary basin on Rayleigh wave propagation from nuclear explosions at Novaya Zemlya (NZ) is shown in Fig.7. As we see, the group velocity for the path NZ-KEVO across the Barents Sea shelf with a thick sedimentary basin is significantly lower than for the model EUS. This fact presents an opportunity for reconnaissance of the sediment thickness preceding active seismic investigations (Levshin and Berteussen 1979; Egorkin et al. 1988).

7 Surface waves: local scale

An interesting application of surface wave seismology is related to the off-shore seismic prospecting for oil and gas. In recent years, the technology of this industry has resulted in significant changes. Instead of streamers floating in the water near the surface, many seismic

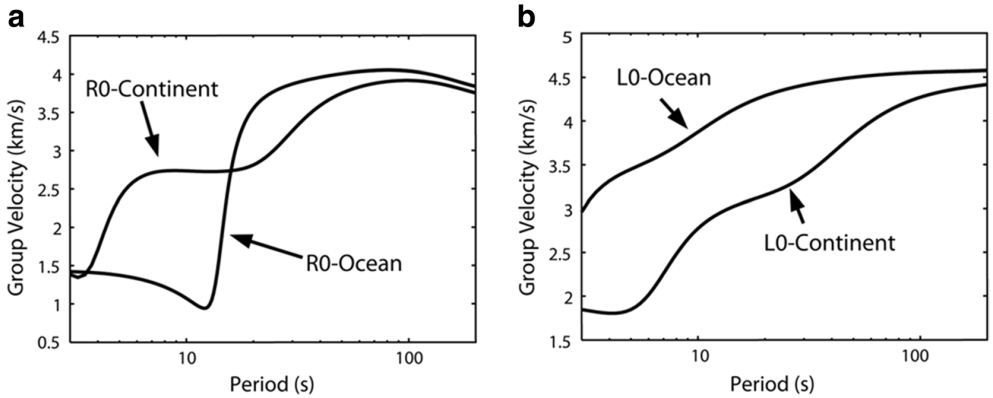

Fig. 4 Comparison of group velocity dispersion for fundamental modes of Rayleigh (**a**) and Love (**b**) waves for typical 1-D continental model AK135 (Kennett et al. 1995) and oceanic model (Herrmann 2013)

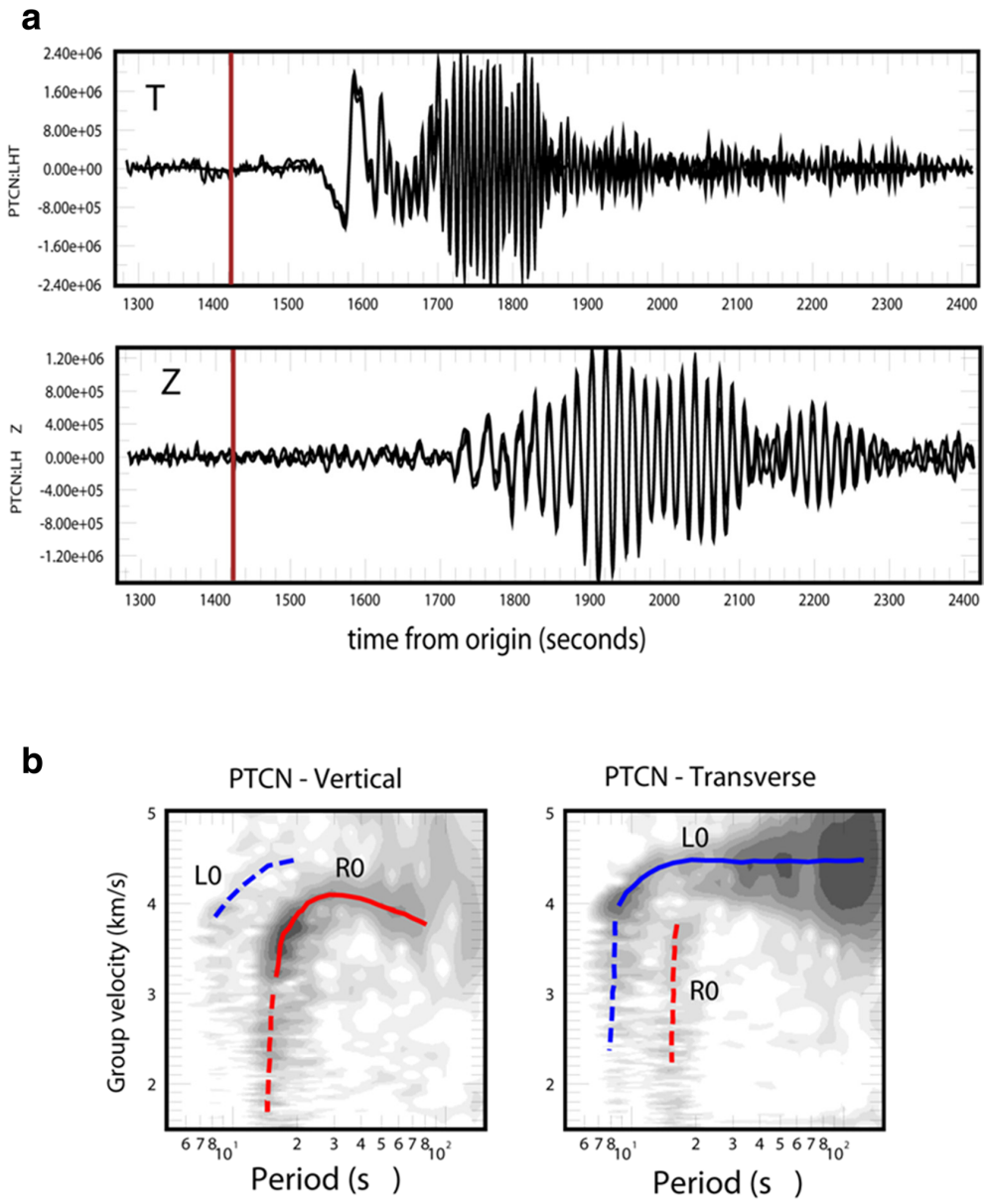

Fig. 5 Seismograms (**a**) and FTAN diagrams (**b**) of vertical and transverse components of surface waves propagating across the Pacific Ocean from the earthquake near the Balleny Islands (close to the Antarctic) (March 25 of 1998, M = 8.1), recorded by the Global Seismic Network (GSN) at the station PTCN (Pitcairn Islands, Great Britain; epicentral distance 3443 km)

crews now use three-component bottom receivers plus hydrophones to record seismic signals generated by air guns. The main goal is to record converted reflected PS waves which are less sensitive to gas saturation. The presence of gas in rocks causes scattering and attenuation of P waves but produces almost no effect on S waves. For these reasons, seismic images obtained using PS reflections are much more focused than standard PP images. However, a serious difficulty in using PS waves is the absence of information about shear velocities near the bottom, which is needed to make static correction of the PS travel times. There is good reason to use surface

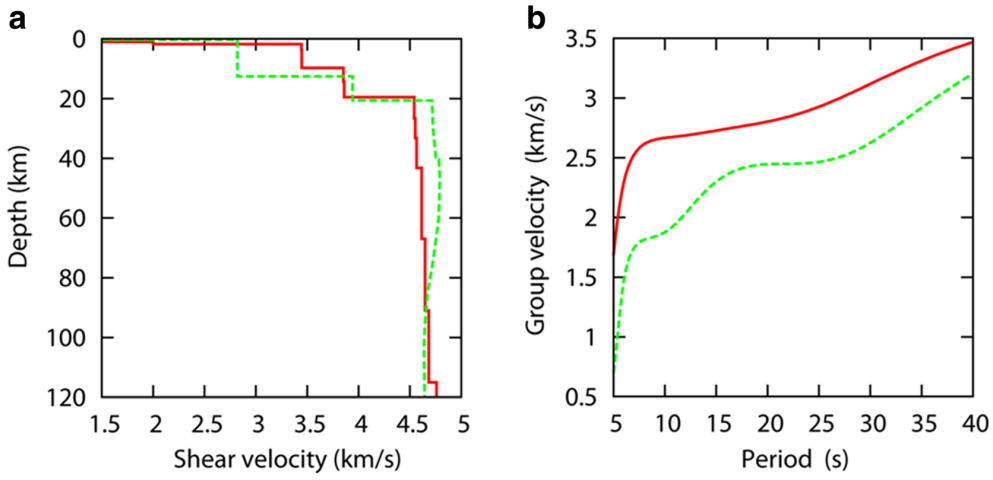

Fig. 6 **a** 1-D models: the continental platform EUS (red) and model with the thick sedimentary basin (green). **b** Comparison of group velocity dispersion for fundamental mode of Rayleigh waves for two models

waves for this purpose since they can be well observed, if the air gun is not too far from the bottom (10–15 m in the case of a very soft bottom, or up to 50–70 m for harder, rocky bottom floors).

Figure 8 provides an example of a record section from a seismic survey near the Louisiana coast in the Mexican Gulf. Records were passed through low-pass filtering to suppress *P* waves and partly suppress PS reflection. We see several groups of slow dispersive waves which are usually called "ground roll" or, in this case, "mud roll". FTAN diagrams for both vertical and horizontal components at the same range of frequencies are shown in Fig. 9.

Theoretical group velocity curves computed from the shallow marine model are plotted over these diagrams. We can distinguish a fundamental (Scholte) wave I_o at the vertical component, and several higher (Rayleigh) modes at the horizontal component. Some of these (such as the first higher mode I_1) are separated in frequency–time space from others; others interfere with so-called guided waves G_1, G_2; these latter are known as quasi-impulsive nondispersive arrivals; *S* is the body shear wave.

Our interpretation is shown in Fig. 10 (Ritzwoller and Levshin 2002). The resulting average profiles obtained by Monte-Carlo inversion are shown in Fig. 11. Note the extremely low velocities of shear waves in the upper 10 m below the bottom (40–50 m/s), with *Vp*/*Vs* ratio on the order of 30! This demonstrates how important static corrections could be for reconciling PP and PS

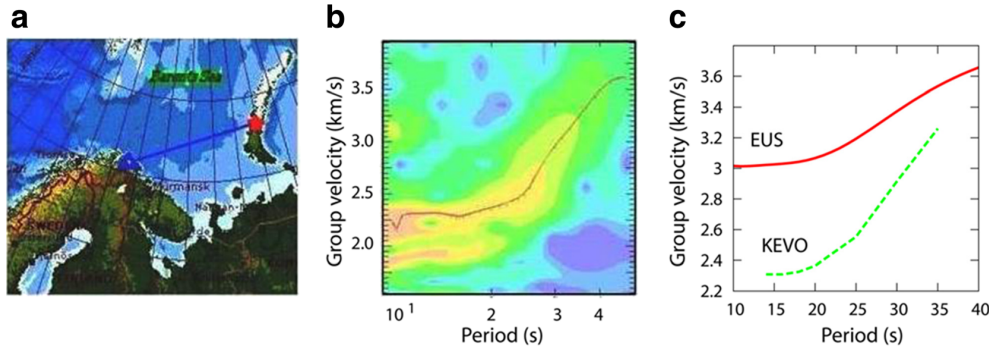

Fig. 7 **a** The map of Northern Europe showing the recording station KEVO in northern Finland, and the test site at Novaya Zemlya (NZ) with corresponding wave path. **b** The raw FTAN diagram of the vertical component at KEVO. **c** Group velocities of Rayleigh waves for paths NZ-KEVO and for the standard continental model EUS with 2 km of dense sediments shown on Fig.6a

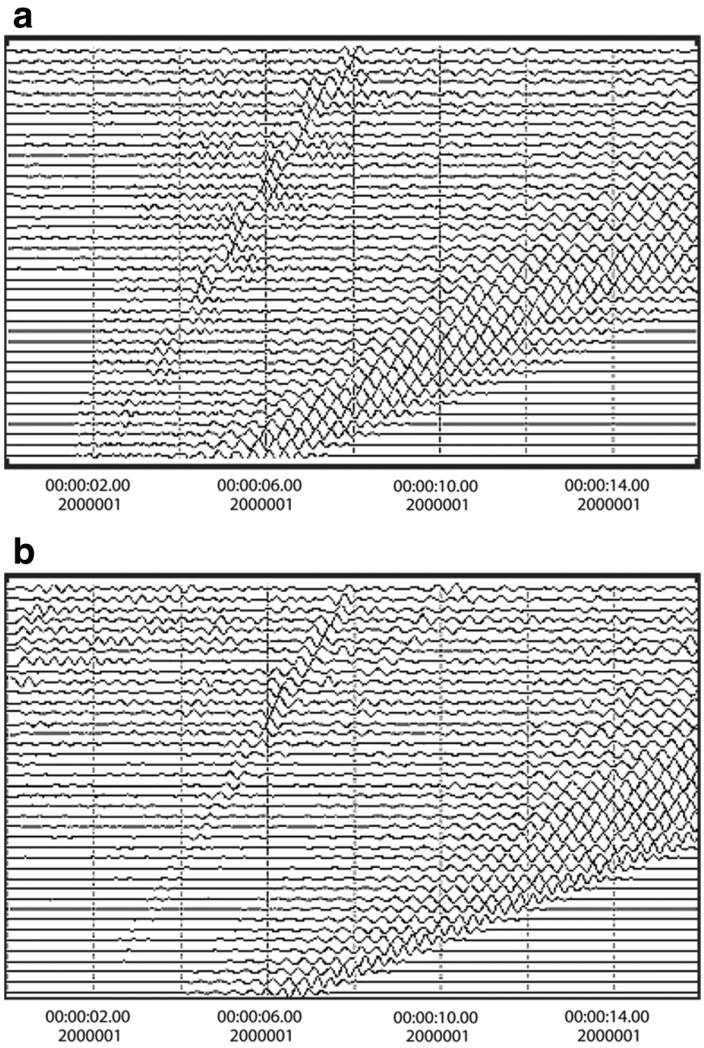

Fig. 8 Example of observed seismic sections at underwater prospecting locations in the Mexican Gulf near the coast of Louisiana. **a** Horizontal component. **b** Vertical component

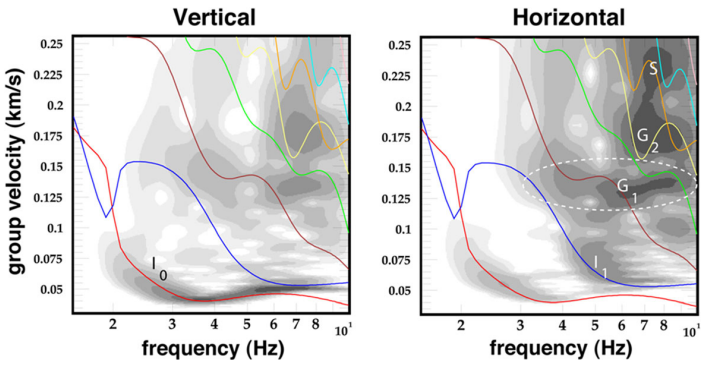

Fig. 9 FTAN diagrams corresponding to a typical seismic record from Fig.8

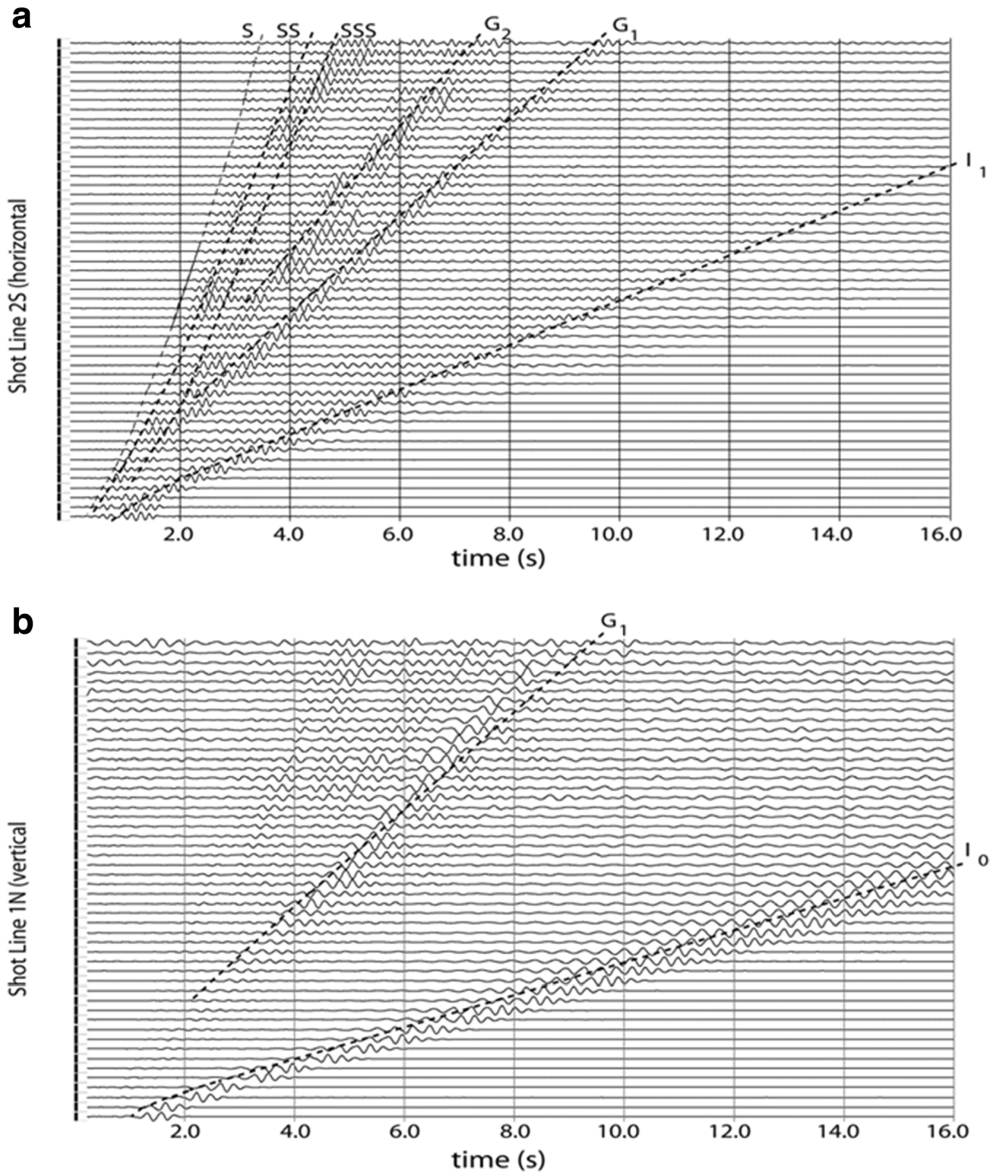

Fig. 10 Interpretation of observed wave forms in terms of modes and waves. **a** Horizontal component. **b** Vertical component

images. As three-component receivers also become common on land, applications of surface waves for these purposes may become more and more important.

Other applications of surface wave seismology on local scale include observations of short-period Rayleigh and Love waves in civil engineering for studying properties of loose sediments and the basements using explosions, mechanical impacts, vibrators, and ambient noise (e.g., Levshin 1962; Gabriels et al. 1987; Park et al. 1999; Xia et al. 1999; Gribler et al. 2016).

8 Higher modes in the Earth's crust

Crustal overtones at periods below 15–20 s present information about crustal structure that, if used together

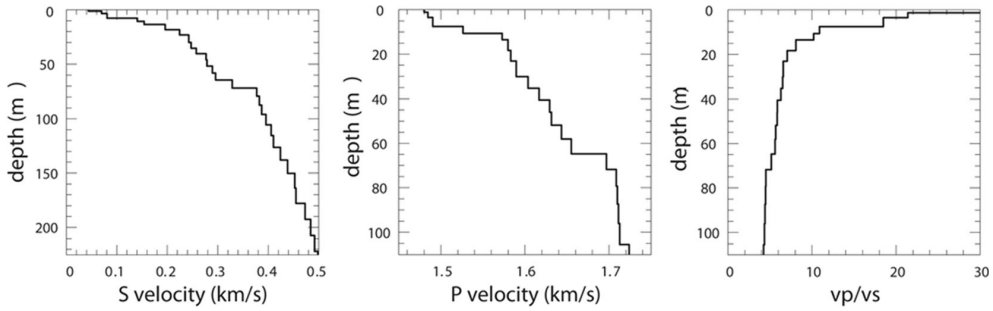

Fig. 11 Vertical profiles obtained as a result of data inversion

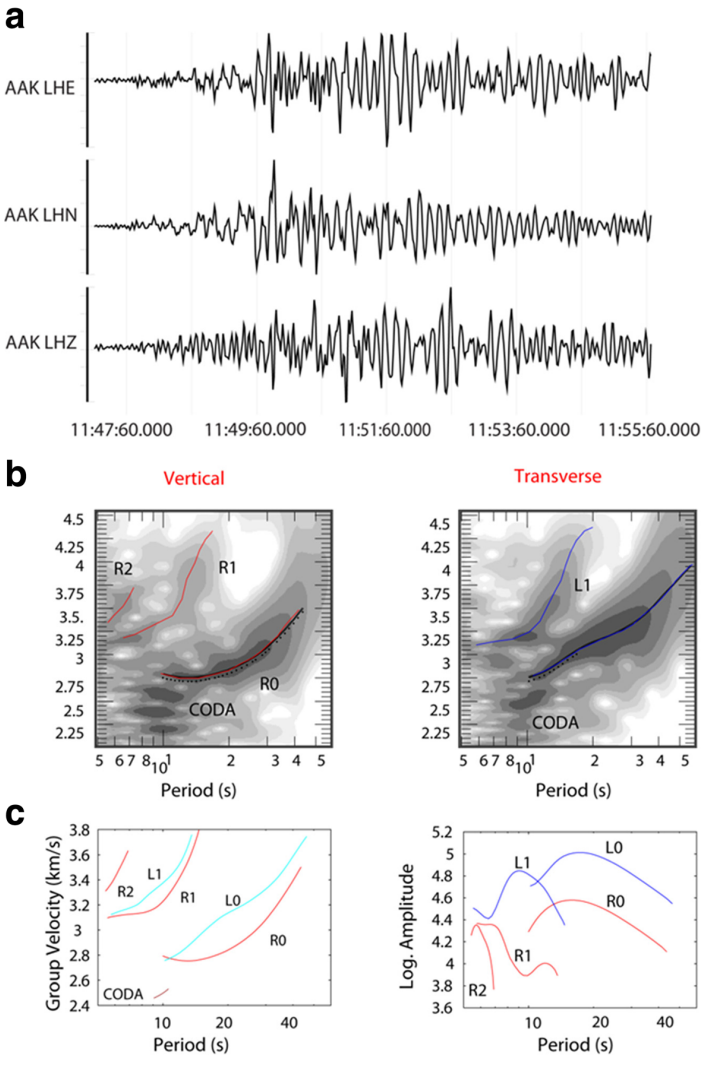

Fig. 12 Rayleigh and Love modes from the event at the Iran-Turkmenistan border on August 4, 1998 (depth 33 km, magnitude Ms = 4.9) at the AAK station (Kyrgyzstan). **a** Records. **b** Raw FTAN diagrams. **c** Group velocities (left) and amplitude spectra (right)

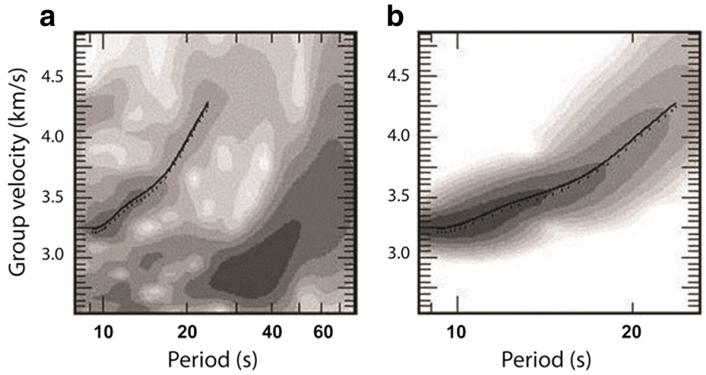

Fig. 13 FTAN diagrams of the Rayleigh waves of the record of event in N. Pakistan on May 10, 1992 (depth 33 km, Ms = 5.6) recorded at BUDO (Tibetan Plateau). **a** Raw FTAN diagram. **b** FTAN diagram for the extracted higher mode

with fundamental mode data, may significantly improve estimates of the structure of the crust and resolution of the underlying mantle. Several studies have demonstrated the observability and usefulness of crustal higher modes (e.g., Oliver and Ewing 1957, 1958; Oliver et al. 1959; Alexander 1962; Oliver 1962; Brune and Dorman 1963; Crampin 1964; Kovach and Anderson 1964; Crampin 1966a, b; Nolet 1975; Crampin and King 1977; Nolet 1977, 1978; Levshin et al. 2005). Higher modes are relatively strong in comparison with fundamental modes for intermediate and deep events. A typical example is shown in Fig. 12. The record of the Ala-Archa station (AAK) near the capital of Kyrgyzstan in Central Asia is shown. Epicentral distance is 1560 km; the path is across the Kopet-Dag Mountains and the Turan and Kazakh plates. The record looks quite complicated. FTAN diagram show very clearly several modes of surface waves and multiple late arrivals labeled CODA. The variability of group velocities and amplitude spectra of all detected modes is quite evident.

Other examples (Figs.13 and 14) demonstrate how the higher mode observations could be used for surface wave tomographic inversion together with fundamental modes. In Fig.13a, FTAN diagram for an event in N. Pakistan on May 10, 1992 (depth 33 km, Ms = 5.6) recorded at BUDO, at epicentral distance 1890 km. (Tibetan Plateau PASSCAL Experiment, 1991–1992, Owens et al. 1993). Both fundamental and first higher modes of Rayleigh waves are shown; the diagram on the right is the filtered diagram for the higher mode used for dispersion measurements.

Figure 14 presents similar diagrams for the location in Southwestern China. The joint inversion of similar measurements reduces the range of acceptable models in both the crust and the mantle and reduces the range of crustal thicknesses while fitting all data acceptably (Levshin et al. 2005).

9 Path deviations

As mentioned earlier, the lateral inhomogeneity of the Earth is responsible for many complications in surface wave propagation. One of these, well documented in

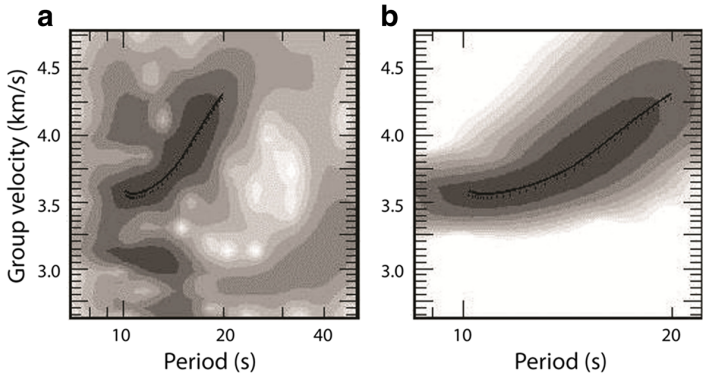

Fig. 14 FTAN diagrams of the Rayleigh waves for the event in the Hindu Kush on 2001 October 27 (depth 96 km, mb = 4.8) recorded at HILE (Himalayan Tubet Nepal PASSCAL Experiment, 2000–2001, Sheehan et al. 2002). Epicentral distance 1880 km. **a** Raw FTAN diagram. **b** FTAN diagram for the extracted higher mode

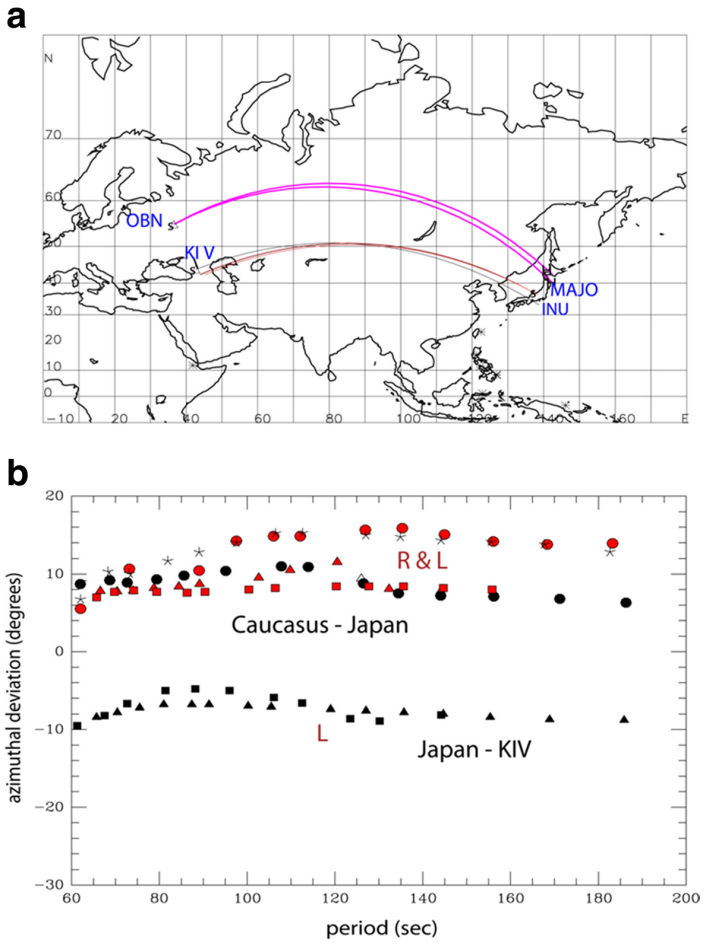

Fig. 15 Azimuthal deviations of Rayleigh and Love waves propagating across Eurasia. **a** Great circle paths to OBN, KIV from Japan and MAJO, INU from Caucasus. **b** Azimuthal deviations along reciprocal paths. The upper group of measurements corresponds to the West-East propagation, the lower one to the East-West propagation. The magnitude of deviations is similar, but their signs are different, indicating for both sets of oppositely traveling waves a deflection to the North

seismic literature, is the deviation of the surface wave path from the shortest (great circle) path between the source and the receiver. There are two techniques for detecting such deviations. One is based on measuring travel time delays of surface wave propagation across the array or dense local network of seismic stations (e.g., Bungum and Capon 1974); the other is the use of three-component records to analyze polarization of surface waves (Lander 1989a; Paulssen et al. 1990; Levshin et al. 1992; Levshin et al. 1994; Laske 1995). Effects of relatively smooth lateral inhomogeneity will manifest themselves in deviation of the vertical plane containing Rayleigh wave particle motion from a plane passing through the great circle epicenter-station. Particle motion in Love waves will be orthogonal to this new plane. Figure 15 shows results of such measurements of surface wave polarization using a modification of FTAN called FTPAN (Frequency–Time Polarization Analysis, Lander 1989b; Levshin et al. 1992).

These measurements were performed for relatively long periods (> 60 s) to prevent Love-Rayleigh interference from distorting the polarization picture. Records of the Russian station (KIV) at N. Caucasus for events near S. Honshu and records of stations in Japan (INU and MAJO) for events at N. Caucasus were used to compare observed anomaly along nearly reciprocal paths. Good agreement between measurements along reciprocal paths can be seen in Fig.15b. Observed Rayleigh and Love waves show significant azimuthal anomalies (up to 10° to the North) caused by an increase of velocities in the upper mantle and thinning of the crust from South to North across Siberia. For more northern paths

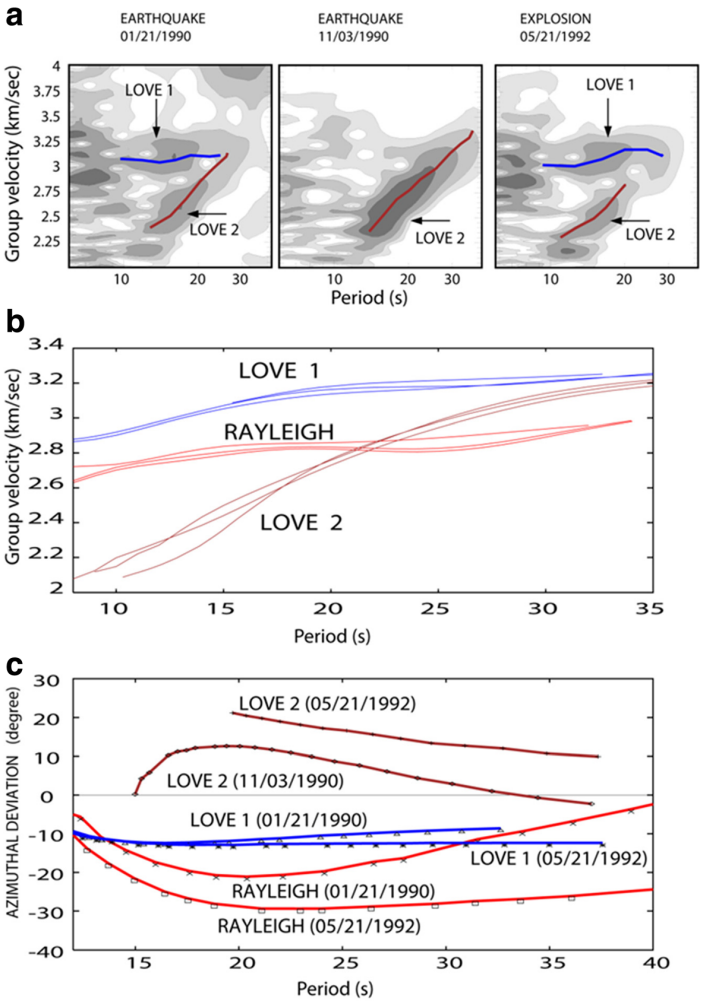

Fig. 16 Group velocities and azimuthal deviations of Rayleigh and Love waves propagating across Central Asia from Lop Nor (China) to Garm (Tadzhikistan). **a** FTAN diagrams. **b** Observed group velocities. **c** Azimuthal deviations from great circle paths. Epicentral distances are ~ 1600 km

between OBN and Japan azimuthal deviations are less significant. It bears mention that most tomographic studies do not take this effect into account. Such effects may be more severe for shorter periods (i.e., shorter wavelengths) resulting in blurring and bias in tomographic images.

10 "Looking for Love in all the wrong places"

This joke belongs to Prof. Jeff Park at Yale University. He discovered the presence of quasi-Love waves at the vertical components of some long-period records and explained them as the effect of anisotropy (e.g., Park 1996; Levin and Park 1998). There are some other examples where Love waves appear at the wrong component due to other reasons, such as multipathing, path deviation (discussed above), and tectonic release.

It is also worthwhile to note that some anomalies of polarization may be caused by anisotropy (Anderson 1961, Crampin 1975; Park 1996; Levin and Park 1998) and that there are no simple rules for discrimination between two factors (lateral inhomogeneity and anisotropy) which influence surface wave polarization. In addition to deviations of the main train of surface waves from the shortest path, we often observed another phenomenon, namely multipathing, in which part of the surface wave energy splits from the main train and propagates on its own, mostly tunneled by some laterally extended low-velocity waveguide

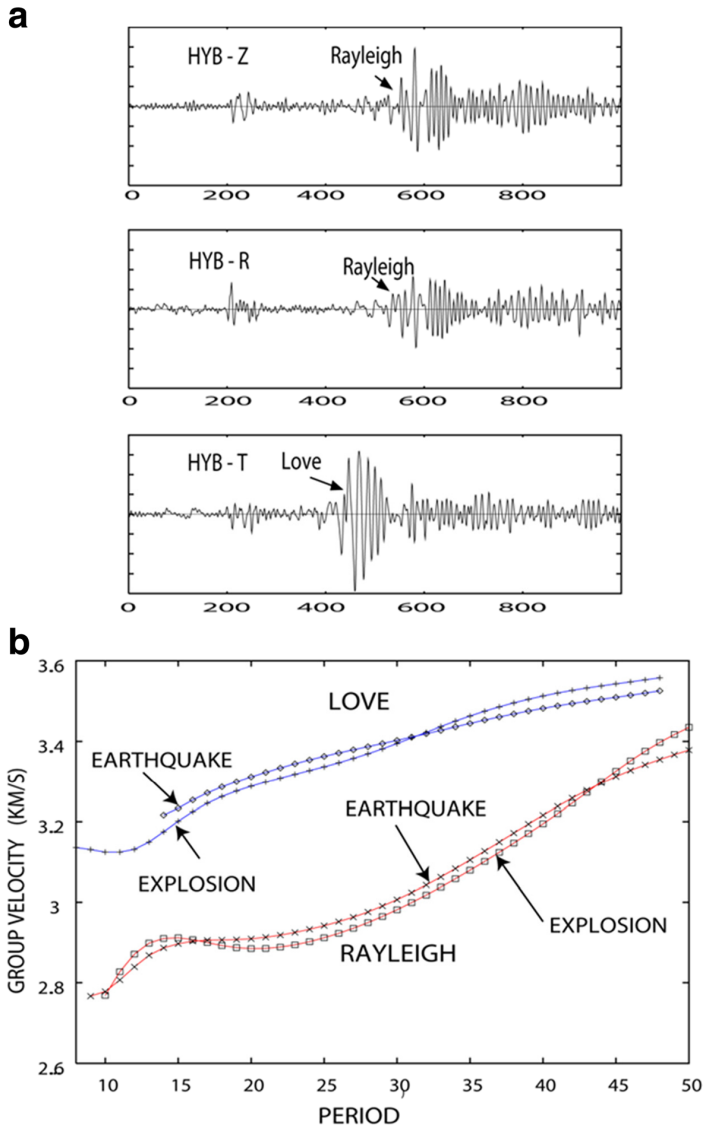

Fig. 17 Propagation of Rayleigh and Love waves from the nuclear explosion and the earthquake from the Lop Nor region (China) to Hyderabad (India). **a** Seismograms for nuclear explosion. **b** Dispersion curves from records of the explosion and earthquake

such as the foredeep of some mountain range, a sedimentary basin, or the oceanic trench near the coast of a continent. Usually, this carries only a short-period part of the surface wave spectrum and, through some yet unknown mechanism, consists predominantly of Love waves. Figure 16 demonstrates such a phenomenon for Love waves propagating from Northwestern China to the Garm (GAR) station in Tajikistan.

The late arrival is a series of Love waves tunneled by the Tarim Basin where thickness of sediments reaches 10–12 km. Naturally, this Love wave train comes much later than a direct arrival (Fig.16a, b) and has a different angle of approach to the station than the direct arrival (Fig.16c). Similar effects were observed in many other observations.

Multipathing also may be caused by reflections of surface waves at some sharp discontinuities (boundaries of crustal blocks, rifts, deep grabens) (e.g., Levshin and Berteussen 1979; Berteussen et al. 1983), or conversion of Love waves into Rayleigh waves at sharp discontinuities.

Theory predicts that Love waves (as SH waves) should not be observed in a laterally homogeneous

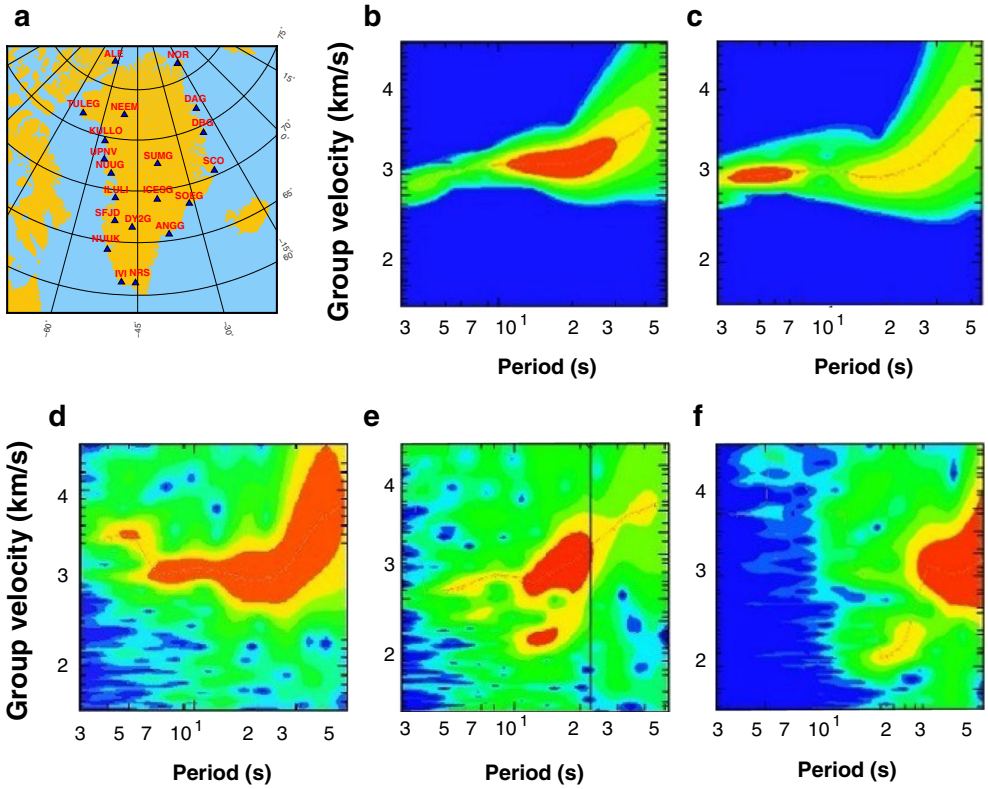

Fig. 18 FTAN diagrams of Rayleigh waves obtained by analysis of ambient noise in Greenland (**a**) map of stations. **b**–**f** FTAN diagrams for different pairs of stations, namely: **b** IVI-SUMG, **c** NEEM-ICEGS, **d** ALE-NEEM, **e** SCO-NOR, and **f** NUUG-ILULI.

Earth if the source is a center of expansion (i.e., dilatation) or a vertical force. Nevertheless, there are excellent long-period Love waves generated by nuclear explosions. There are some other examples where Love waves appear at the wrong component due to other reasons, such as multipathing and path deviation (discussed above) and tectonic release.

Fig. 17a shows records of vertical, radial, and transverse components for the nuclear explosion at Lop Nor (Northwestern China) obtained at the GEOSCOPE station HYB in Central India. A strong Love wave is a dominant feature of these records. Figure 17b demonstrates that surface wave group velocities observed at HYB for this explosion and for the earthquake of November 3, 1990 near Lop Nor are very similar. This implies that Love waves from the explosion are generated very close to the source and do not result from Rayleigh–Love coupling due to lateral structures along the wave path. Observations at other stations, at quite different directions from Lop Nor, and for another set of explosions and earthquakes are similar (Levshin and Ritzwoller 1995; Bukchin et al. 2000).

The traditional explanation of these phenomena is tectonic release provoked by an explosion in a prestressed area. Numerous papers describe and explain tectonic release (e.g., Press and Archambeau 1962; Archambeau and Sammis 1970; Harkrider et al. 1994) The interest in such phenomena is due to the fact that they make it more difficult to distinguish between earthquakes and underground nuclear explosions using a well-known m_b:M_S discriminant (e.g., Steven and Day 1985). This discriminant is based on relative differences between body wave and surface magnitudes for explosions and earthquakes: due to the smaller size of the source zone and the shorter duration, explosions are "better" generators of *P* waves than of surface waves. Tectonic release diminishes these differences. However, the absence of an isotropic component in earthquake

radiation and a very small depth of the equivalent source of tectonic release from an explosion may help to discriminate these events (Bukchin et al. 2000).

11 Surface waves extracted from ambient seismic noise

Recently, numerous studies of ambient seismic noise, primarily following the pioneering work by (Shapiro et al. 2005) and a detailed description of the corresponding methodology by (Bensen et al. 2007), have presented numerous examples of the different phenomenology of surface waves extracted from noise. We demonstrate here some examples of such analysis based on recordings obtained by the Greenland Ice Sheet Monitoring Network (GLISN, Clinton et al. 2014) (Fig.18).

The prevailing results characterize Rayleigh wave propagation in the continental crust. Typical examples are shown in Fig.18b–f. Figure 18b presents a FTAN diagram in the period for the range of 5–40 s for stations IVI-SUMG with an interstation distance of 1335 km. The path crosses the central and southern parts of the Greenland shield. Figure 18c comprises a similar diagram for stations NEEM-ICESG with interstation distance of 998 km with paths crossing central and northern parts of the shield. A different type of FTAN diagram is shown in Fig. 18d–f.

The diagram for the path "ALI-NEEM", with a length of 603 km (Fig.18d), demonstrates a strong fundamental mode of Rayleigh wave with higher velocities at long periods due to the thinner crust at the northern rim of Greenland, as well as the first higher mode at short periods 3–6 s. Figure 18e demonstrates a more complicated wave pattern for the path between NOR and SCO stations (1248 km) following along the eastern coast of Greenland. The fundamental mode follows the shield path but its short-period portion is much weaker than at periods of 12–20 s.

Here, the effect of multipathing is also seen in the strong signal at later times caused by propagation in loose sediments under the Atlantic Ocean shelf. Figure 18f is for a short path between NUUG and ILULI station (276 km) along the western coast of the island where only short periods of the spectrum are shown.

The demonstrated examples do not cover, of course, all possible situations which could be encountered in the ambient noise analysis in different regions around the Earth.

12 Conclusions

The description of surface wave phenomenology is based on cases encountered by the authors in their long-term investigation of surface wave excitation, propagation, and interpretation. It demonstrates the variability of observed wave patterns across various applications and the difficulties which could challenge their interpretation.

Acknowledgements The facilities of the IRIS Data Management System, and specifically the IRIS Data Management Center, were used to access the waveform and metadata required in this study. The IRIS DMS is funded through the National Science Foundation of the USA and specifically the GEO Directorate through the Instrumentation and Facilities Program of the National Science Foundation under Cooperative Agreement EAR-0552316.

We are grateful for permission to use proprietary data granted to us by Fairfield Industries, Unocal, and Western Geophysical in examples related to sea experiments. We are thankful to anonymous reviewer for his detailed comments, Mr. P.F. Spencer for help in editing manuscript, and Mr. L.J. Brioso (Springer) for assistance in publication.

References

Alexander SS (1962) A study of the normal modes of surface waves across the Western United States. J Geophys Res 67: 3537–3538

Anderson DL (1961) Elastic wave propagation in layered anisotropic media. J Geophys Res 66(9):2953–2963. https://doi.org/10.1029/JZ066i009p02953

Archambeau CB, Sammis C (1970) Seismic radiation from explosions in prestressed media and the measurement of tectonic stress in the Earth. Rev Geophys 8(3):473–499

Bensen GD, Ritzwoller MH, Barmin MP, Levshin AL, Lin F, Moschetti MP, Shapiro NM, Yang Y (2007) Processing seismic ambient noise data to obtain reliable broad-band surface wave dispersion measurements. Geophys J Int 169:1239-1260, https://doi.org/10.1111/j.1365-246X.2007.03374.x

Berteussen K-A, Levshin AL, and LI Ratnikova (1983) Regional studies on the crust in Eurasia with surface waves recorded by the NORSAR group. In Mathematical models of the structure of the earth and the earthquake prediction, Comput. Seismology, 14. Allerton press, New York, 106–116

Brune J, Dorman J (1963) Seismic waves and Earth structure in the Canadian shield. Bull Seismol Soc Am 53:167–210

Bukchin BG, Mostinsky AZ, Egorkin AA, Levshin AL, and Ritzwoller MH (2000) Isotropic and nonisotropic components of earthquakes and nuclear explosions on the Lop Nor Test Site, China. Pure Appl Geophys, Special volume on CTBT Monitoring, Surface Waves 158(8):1497–1515

Bungum H, Capon J (1974) Coda pattern and multipath propagation of Rayleigh waves at NORSAR. Phys Earth Planet Inter 9:11–127

Cara M (1973) Filtering of dispersed wave trains. Geophys J Roy Astron Soc 33(1):65–80. https://doi.org/10.1111/j.1365-246X.1973.tb03415.x

Clinton et al (2014) Seismic network in Greenland monitors earth and ice system. Eos 95(2):13–24. https://doi.org/10.1002/2014EO020001

Crampin S (1964) Higher modes of seismic surface waves: preliminary observations. Geophys J Roy Astron Soc 9:35–37

Crampin S (1966a) Higher modes of seismic surface waves: propagation in Eurasia. Bull Seismol Soc Am 56:1227–1239

Crampin S (1966b) Higher-mode seismic surface waves from atmospheric nuclear explosions over Novaya Zemlya. J Geophys Res 71(12):2951–2958. https://doi.org/10.1029/JZ071i012p02951

Crampin S (1975) Distinctive particle motion of surface waves as a diagnostic of anisotropic layering. Geophys J Roy Astron Soc 40(2):177–186. https://doi.org/10.1111/j.1365-246X.1975.tb07045.x

Crampin S, King D (1977) Evidence for anisotropy in the upper mantle beneath Eurasia from the polarization of higher mode seismic surface waves. Geophys J Roy Astron Soc 49(1):59–85. https://doi.org/10.1111/j.1365-246X.1977.tb03701.x

Dziewonski AM, Anderson DL (1981) Preliminary Reference Earth Model. Phys Earth Planet Inter 25:297–356

Dziewonski AM, Bloch S, Landisman M (1969) A technique for the analysis of transient seismic signals. Bull Seismol Soc Am 59:427–444

Dziewonski AM, Mills J, Bloch S (1972) Residual dispersion measurements: a new method of surface wave analysis. Bull Seismol Soc Am 62:129–139

Egorkin AA, Levshin AL, Yakobson AN (1988) Study of the deep structure of the Barents Sea shelf by seismic surface waves. In: Numerical modeling and analysis of geophysical processes, Comput. Seismology, vol. 20, Allerton Press, New York, pp 197–201

Gabriels P, Snieder R, Nolet G (1987) In situ measurements of shear velocity in sediments with higher mode Rayleigh waves. Geophys Prospect 35:187–196

Gribler G, Liberty LM, Mikesell TD, Michaels P (2016) Isolating retrograde and prograde Rayleigh-wave modes using a polarity mute. Geophysics 81(5):V379–V385. https://doi.org/10.1190/geo2015-0683.1

Harkrider DG, Stevens JL, Archambeau CB (1994) Theoretical Rayleigh and Love waves from an explosion in prestressed source regions. Bull Seismol Soc Am 84:1410–1442

Herrmann RB (2013) Computer programs in seismology: an evolving tool for instruction and research. Seismol Res Lett 84(6):1081–1088. https://doi.org/10.1785/0220110096

Kennett BLN, Engdahl ER, Buland R (1995) Constraints on seismic velocities in the earth from travel times. Geophys J Int 122(1):108–124. https://doi.org/10.1111/j.1365-246X.1995.tb03540.x

Kovach RL, Anderson DL (1964) Higher mode surface waves and their bearing on the structure of the earth's mantle. Bull Seismol Soc Am 54:161–182

Lander AV (1989a) Recording, identification, and measurements of surface wave parameters. In Seismic surface waves a laterally inhomogeneous Earth. Keilis-Borok VI (Ed) Kluwer Publ, Dordrecht, pp 129–182

Lander AV (1989b) Dispersion characteristics of Rayleigh waves on the Asiatic Arctic shelf and structural features of the Laptev Sea. In: Problems of Seismological Information Science, Comput Seismology, vol 21, Allerton Press, New York, pp 142–145

Laske G (1995) Global observation of-great circle propagation of long period surface waves. Geophys J Int 123(1):245–259. https://doi.org/10.1111/j.1365-246X.1995.tb06673.x

Levin V, Park J (1998) Quasi-Love phases between Tonga and Hawaii: observations, simulations and explanations. J Geophys Res 103(B10):24321–24331. https://doi.org/10.1029/98JB02342

Levshin AL (1962) Propagation of surface waves in loose sediments. Izvestia Acad Nauk SSSR Ser Geofis 12:1749–1763 (in Russian)

Levshin AL, Berteussen K-A (1979) Anomalous propagation of surface waves in the Barents Sea as inferred from NORSAR recordings. Geophys J Roy Astron Soc 56:97–118.20

Levshin AL, Ritzwoller MH (1995) Characteristics of surface waves generated by events on and near the Chinese nuclear test site. Geophys Journal Int 123(1):131–148. https://doi.org/10.1111/j.1365-246X.1995.tb06666.x

Levshin AL, Ritzwoller MH (2001) Automated detection, extraction, and measurement of regional surface waves. PAGEOPH 158(8):1531–1545

Levshin AL, Pisarenko VF, Pogrebinsky GA (1972) On a frequency-time analysis of oscillations. Ann Geophys 28:211–218

Levshin AL, Yanovskaya TB, Lander AV, Bukchin BG, Barmin MP, Ratnikova LI, Its, E.N. (Ed. V.I. Keilis-Borok) (1989) Seismic surface waves a laterally inhomogeneous Earth. Kluwer Publ, Dordrecht, pp 129–182

Levshin AL, Ratnikova LI, Berger J (1992) Peculiarities of surface wave propagation across Central Eurasia. Bull Seism Soc Am 82:2464–2493

Levshin AL, Ritzwoller MH, Ratnikova LI (1994) The nature and cause of polarization anomalies of surface waves crossing northern and central Eurasia. Geophys J Int 117(3):577–590. https://doi.org/10.1111/j.1365-246X.1994.tb02455.x

Levshin AL, Ritzwoller MH, Resovsky JS (1999) Source effects on surface wave group travel times and group velocity maps. Phys Earth Planet Inter 115(3-4):293–312. https://doi.org/10.1016/S0031-9201(99)00113-2

Levshin AL, Ritzwoller MH, Shapiro NM (2005) The use of crustal higher modes to constrain crustal structure across Central Asia. Geophys J Int 160:1–12

Nolet G (1975) Higher Rayleigh modes in Western Europe. Geophys Res Lett 2(2):60–62. https://doi.org/10.1029/GL002i002p00060

Nolet G (1977) The upper mantle under Western Europe inferred from the dispersion of Rayleigh modes. J Geophys 43:265–285

Nolet G (1978) Simultaneous inversion of seismic data. Geophys J R Astron Soc 55(3):679–691. https://doi.org/10.1111/j.1365-246X.1978.tb05936.x

Oliver J (1962) A summary of observed surface wave dispersion. Bull Seismol Soc Am 52:81–86

Oliver J, Ewing M (1957) Higher modes of continental Rayleigh waves. Bull Seismol Soc Am 47:187–204

Oliver J, Ewing M (1958) Normal modes of continental Rayleigh waves. Bull Seismol Soc Am 48:33–49

Oliver J, Dorman J, Sutton G (1959) The second shear mode of continental Rayleigh waves. Bull Seismol Soc Am 49:379–389

Owens TJ, Randall GE, Wu FT, Zeng RS (1993) PASSCAL instrument performance during the Tibetan plateau passive seismic experiment. Bull Seismol Soc Am 83:1959–1970

Park J (1996) Surface waves in layered anisotropic structures. Geophys J Int 126(1):173–183. https://doi.org/10.1111/j.1365-246X.1996.tb05276.x

Park CB, Miller RD, Xia J (1999) Multichannel analysis of surface waves. Geophysics 64(3):800–808. https://doi.org/10.1190/1.1444590

Paulssen H, Levshin AL, Lander AV, Snieder R (1990) Time and frequency dependent polarization analysis: anomalous surface wave observations in Iberia. Geophys J Int 103:483–496

Press F, Archambeau CG (1962) Release of tectonic strain by underground nuclear explosions. J Geophys Res 67(1):337–343. https://doi.org/10.1029/JZ067i001p00337

Ritzwoller MH, Levshin AL (1998) Surface wave tomography of Eurasia: group velocities. J Geophys Res 103(B3):4839–4878. https://doi.org/10.1029/97JB02622

Ritzwoller MH, Levshin AL (2002) Estimating shallow shear velocities with marine multi-component seismic data. Geophysics 67(6):1991–2004

Ritzwoller MH, Levshin AL, Smith SS, and Lee CS (1995) Making accurate continental broadband surface wave measurements. Proceedings of the 17th Seismic Research Symposium on Monitoring and Comprehensive Ban Treaty Phillips Laboratory 482–491

Russell DW, Herrmann RB, Hwang H (1988) Application of frequency-variable filters to surface wave amplitude analysis. Bull Seismol Soc Am 78:339–354

Shapiro NM, Ritzwoller MH (2002) Monte-Carlo inversion for a global shear velocity model of the crust and upper mantle. Geophys J Int 151(1):88–105. https://doi.org/10.1046/j.1365-246X.2002.01742.x

Shapiro NM, Campillo M, Stehly L, Ritzwoller MH (2005) High resolution surface wave tomography from ambient seismic noise. Science 307(5715):1615–1618. https://doi.org/10.1126/science.1108339

Sheehan AF et al (2002) Himalayan Nepal Tibet broadband seismic experiment (HIMNT). EOS Trans Am Geophys Un 83, Fall Meet. Suppl., Abstract:S61D–S611

Steven JL, Day SM (1985) The physical basis of mb:Ms and variable frequency magnitude methods for earthquake/explosion discrimination. J Geophys Res Solid Earth 90(B4):3009–3020. https://doi.org/10.1029/JB090iB04p03009

Vernon F (1994) The Kyrgyz seismic network. IRIS Newsletter, v. XIII, No. 2

Xia J, Miller RD, Park CB (1999) Estimation of near-surface shear-wave velocity by inversion of Rayleigh waves. Geophysics 64(3):691–700. https://doi.org/10.1190/1.1444578